

Spatial entanglement of paired photons generated in cold atomic ensembles

Clara I. Osorio,^{1,*} Sergio Barreiro,¹ Morgan W. Mitchell,¹ and Juan P. Torres^{1,2}

¹*ICFO-Institut de Ciències Fotoniques, Mediterranean Technology Park, Avenue del Canal Olímpic s/n, 08860, Castelldefels, Barcelona, Spain*

²*Departamento Signal Theory and Communications, Campus Nord D3, Universitat Politècnica de Catalunya, 08034, Barcelona, Spain*
(Received 21 April 2008; published 3 November 2008)

Cold atomic ensembles can mediate the generation of entanglement between pairs of photons. Photons with specific directions of propagation are detected, and the entanglement can reside in any of the degrees of freedom that describe the whole quantum state of the photons: polarization, spatial shape, or frequency. We show that the direction of propagation of the generated photons determines the spatial quantum state of the photons and, therefore, the amount of entanglement generated. When photons generated in different directions are combined, this spatially distinguishing information can degrade the quantum purity of the polarization or frequency entanglement.

DOI: 10.1103/PhysRevA.78.052301

PACS number(s): 03.67.Mn, 42.50.Dv, 42.65.Lm

I. INTRODUCTION

The generation of pairs of photons with controllable entanglement is one of the paramount goals in quantum optics. These states of light are used as tools to implement new protocols with quantum-enhanced capabilities [1,2]. Although spontaneous parametric down-conversion (SPDC) is by far the most widely used source for generating entangled paired photons, in the last few years, many interesting schemes have been proposed that make use of Raman transitions on atomic ensembles to generate entangled pairs of photons.

In these schemes, a classical pump (write) beam impinges on an ensemble of N atoms—for instance, rubidium or cesium—and it induces the emission of, at most, a single photon (*Stokes photon*) from one of the atoms [3]. Such emission generates a collective atomic excitation that can be read by a control beam, which induces the emission of another photon (*anti-Stokes photon*) entangled with the Stokes photon. Quantum correlations mediated by the generation of a collective excitation in an ensemble of atoms have been observed in polarization [4], time-frequency [5], and orbital angular momentum (OAM) [6] degrees of freedom.

In a typical experimental configuration (as shown in Fig. 1), the Stokes and anti-Stokes photons are detected in a small section of the full set of directions where the Stokes and anti-Stokes photons can be emitted [3,7,8]. In most cases, such detection modes are nearly collinear ($\sim 2^\circ - 3^\circ$) with the direction of propagation of counterpropagating pump and control beams [9]. But other situations can be considered as well, as is the case of transverse emitting configurations, where the Stokes and anti-Stokes photons propagate transversally to the pump and control beams [5].

The question arises if the specific noncollinear configuration used might affect the amount and nature of the generated entanglement. This is especially important when Stokes and anti-Stokes photons selected at different angles are combined to generate new types of entangled states in a multidimen-

sional Hilbert space [10]. Paired photons generated in different directions might show *azimuthal distinguishing information*—i.e., different spatial quantum correlations and amount of entanglement. This spatial distinguishing information, for instance, can severely degrade the quality of polarization entanglement, since the full quantum state that describes the entangled photons is a nonseparable mixture of polarization and spatial variables. Here we show that this is the case for highly noncollinear configurations. The direction of propagation of the pump and control beams determine a preferred direction, so configurations where the Stokes and anti-Stokes photons are selected at different angles with respect to this direction might show different quantum properties. This is reminiscent of what it happens in noncollinear SPDC configurations [11–13].

II. QUANTUM STATE OF THE STOKES+ANTISTOKES PAIR OF PHOTONS

The basic setup considered is shown in Fig. 1. An ensemble of N identical cold atoms is trapped in a magneto-optical trap (MOT). The atoms have a Λ -type level configuration, with two hyperfine ground states $|g\rangle$ and $|s\rangle$ and one excited state $|e\rangle$. All atoms are initially in the ground state $|g\rangle$. Two counterpropagating continuous wave laser beams are used to induce the emission of pairs of photons, the Stokes (s) and anti-Stokes (as) photons.

A weak Gaussian pump beam, whose shape in the transverse wave number $\mathbf{q}=(q_x, q_y)$ domain is $E_p(q_x, q_y)$, propagates in the \hat{z} direction. The action of the pump beam, which is far detuned from the $|g\rangle \rightarrow |e\rangle$ transition, results in a small probability of exciting one atom of the cloud and generating by spontaneous Raman scattering one Stokes photon propagating in the direction \hat{z}_s , which forms an angle $\varphi_s = \varphi$ with respect to the \hat{z} direction. The control beam \mathcal{E}_c , which is also far detuned from the $|s\rangle \rightarrow |e\rangle$ transition, propagates in the $-\hat{z}$ direction, resulting in the generation of an anti-Stokes photon propagating in the direction \hat{z}_{as} , which forms an angle $\varphi_{as} = \pi - \varphi$ with respect to the \hat{z} direction.

Energy conservation implies $\omega_p^0 + \omega_c^0 = \omega_s^0 + \omega_{as}^0$, and the phase-matching conditions impose $k_p^0 - k_c^0 = k_s^0 \cos \varphi_s$

*clara.ines.osorio@icfo.es

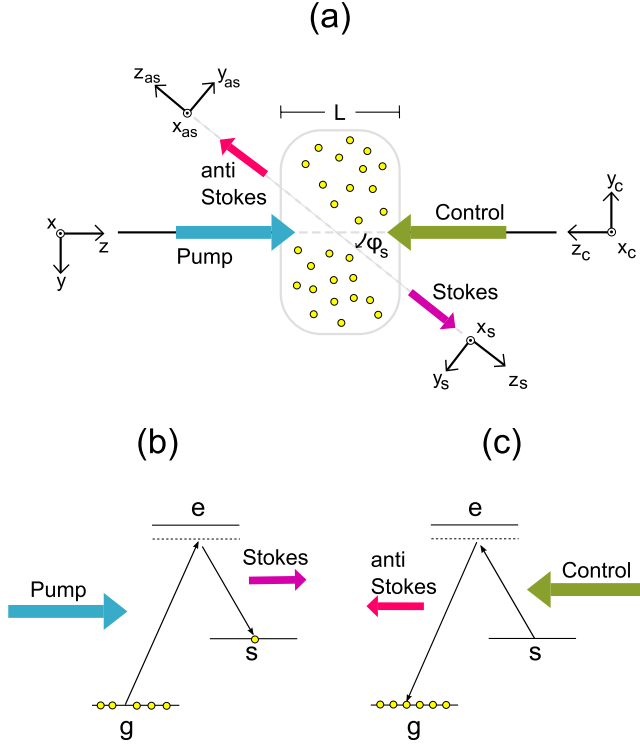


FIG. 1. (Color online) General configuration. (a) Sketch of the geometric configuration. (b) (c) Level structure of the atoms that form the atomic cloud.

$-k_{as}^0 \cos \varphi_{as}$ and $k_s^0 \sin \varphi_s = k_{as}^0 \sin \varphi_{as}$, where ω_i^0 ($i=p, c, s, as$) are the central angular frequencies and k_i^0 are the corresponding wave numbers at the central frequencies. We now consider $D2$ hyperfine transitions in ^{87}Rb . If the pump and control beams have the same frequency [5], then the phase-matching conditions allow any angle of emission $\varphi_{as} = \pi - \varphi$ (always that it is not forbidden by the transition matrix elements), since one then has $\omega_s^0 \simeq \omega_{as}^0$ and $k_s^0 \simeq k_{as}^0$.

In order to describe the quantum state of the Stokes photon, we make use of more convenient transverse wave-vector coordinates $\mathbf{q}_s = (q_s^x, q_s^y)$ [14], which are defined as $q_x = q_s^x$ and $q_y = q_s^y \cos \varphi_s - k_s \sin \varphi_s$, with k_s being the longitudinal wave number of the Stokes photon—similarly for the anti-Stokes photon, which propagates in the \hat{z}_{as} direction with longitudinal wave vector k_{as} and transverse wave vector $\mathbf{q}_{as} = (q_{as}^x, q_{as}^y)$.

Generation of Stokes and anti-Stokes photons can be accurately described by means of (a) two coupled equations in the slowly varying envelope approximation for the Stokes and anti-Stokes electric fields [15] or, alternatively, (b) making use of an effective Hamiltonian of interaction and first-order perturbation theory [16]. In this paper, we choose this second option.

If we assume coherent states for the control and pump beams, with coherent-state amplitudes \mathcal{E}_c and \mathcal{E}_p , respectively, the effective Hamiltonian in the interaction picture, which describes the photon-atom interaction, can be written as

$$H_I = \epsilon_0 \int dV \chi^{(3)} \mathcal{E}_{as}^- \mathcal{E}_s^- \mathcal{E}_c \mathcal{E}_p + \text{H.c.}, \quad (1)$$

where the electric field operator is written

$$\mathcal{E}_s^+(\mathbf{x}_s, z_s, t) = \int d\omega_s d\mathbf{q}_s a_s(\omega_s, \mathbf{q}_s) \times \exp\{ik_s z_s + i\mathbf{q}_s \cdot \mathbf{x}_s - i\omega_s t\}. \quad (2)$$

Here a_s is the annihilation operator of a Stokes photon with frequency ω_s and transverse wave number \mathbf{q}_s and $\mathbf{x}_s = (x_s, y_s)$ is the transverse position vector for the Stokes photon. A similar expression can be written for the electric field operator \mathcal{E}_{as}^+ , with frequency ω_{as} and transverse wave number \mathbf{q}_{as} .

For nonresonant pump and control beams, the effective nonlinearity $\chi^{(3)}$ does not depend on the intensity of the control and pump beams [15]. The distribution of atoms in the cloud is assumed to be Gaussian, so the effective nonlinearity $\chi^{(3)}$ can be written as

$$\chi^{(3)}(x, y, z) \propto \exp\left[-\frac{x^2 + y^2}{R^2} - \frac{z^2}{L^2}\right], \quad (3)$$

where R is the size of the cloud of atoms in the transverse plane (x, y) and L is the size in the longitudinal direction.

The spatial quantum state of the generated pair of photons, at first order of perturbation theory, is $|\Psi\rangle = \int d\mathbf{q}_s d\mathbf{q}_{as} \Phi(\mathbf{q}_s, \mathbf{q}_{as}) |\mathbf{q}_s\rangle_s |\mathbf{q}_{as}\rangle_{as}$, where the mode function Φ of the two photon state is written

$$\begin{aligned} \Phi(\omega_s, \omega_{as}, \mathbf{q}_s, \mathbf{q}_{as}) &= \int d\mathbf{q}_p \mathbf{q}_c E_p(\mathbf{q}_p) E_c(\mathbf{q}_c) \\ &\times \exp(-\Delta_0^2 R^2/4 - \Delta_1^2 R^2/4 - \Delta_2^2 L^2/4), \end{aligned} \quad (4)$$

where

$$\Delta_0 = q_s^x + q_{as}^x,$$

$$\Delta_1 = (k_s - k_{as}) \sin \varphi + (q_s^y - q_{as}^y) \cos \varphi,$$

$$\Delta_2 = k_p - k_c - (k_s + k_{as}) \cos \varphi + (q_s^y - q_{as}^y) \sin \varphi, \quad (5)$$

and the longitudinal wave vector of the pump beam is written $k_p = [(\omega_p n_p / c)^2 - \Delta_0^2 - \Delta_1^2]^{1/2}$, n_p is the refractive index at the pump beam wavelength, and c is the velocity of light in vacuum. Due to the narrow bandwidth (\sim GHz) of the generated Stokes and anti-Stokes photons [5], the spatial shape of the mode function Φ can be analyzed making the substitution $\omega_s = \omega_s^0$ and $\omega_{as} = \omega_{as}^0$.

For the sake of clarity, let us consider that the control and pump beams are Gaussian beams with the same beam waist w_0 (at the center of the cloud $z=0$). Gaussian spatial filters with width w_1 describe the effect of the unavoidable spatial filtering produced by the specific optical detection system used, so that $1/(k_s^0 w_1)$ can be considered as the angular acceptance of the single-photon detection system. In most experimental configurations, $w_1 \sim 50\text{--}150 \mu\text{m}$ and the length of the cloud is a few millimeters long or less. The pump

beam waist is typically 200–500 μm . Therefore, the Rayleigh ranges of pump and of Stokes and anti-Stokes modes, $L_p = \pi w_0^2/\lambda_p$ and $L_{s,as} = \pi w_1^2/\lambda_{s,as}$, fulfill $L \ll L_p, L_{s,as}$. We can thus neglect the transverse wave-number dependence of all longitudinal wave vectors in Eqs. (4) and (5).

Under these conditions, the mode function Φ can be written as

$$\begin{aligned} \Phi(\mathbf{q}_s, \mathbf{q}_{as}) &= \frac{(ABCD)^{1/4}}{\pi} \\ &\times \exp\left\{-\frac{A}{4}(q_s^x + q_{as}^x)^2 - \frac{B}{4}(q_s^x - q_{as}^x)^2\right\} \\ &\times \exp\left\{-\frac{C}{4}(q_s^y + q_{as}^y)^2 - \frac{D}{4}(q_s^y - q_{as}^y)^2\right\}, \quad (6) \end{aligned}$$

where

$$\begin{aligned} A &= \frac{w_0^2 R^2}{2R^2 + w_0^2} + \frac{w_1^2}{2}, \\ B &= w_1^2/2, \\ C &= w_1^2/2, \\ D &= \frac{w_0^2 R^2 \cos^2 \varphi}{2R^2 + w_0^2} + L^2 \sin^2 \varphi + \frac{w_1^2}{2}. \quad (7) \end{aligned}$$

The state is normalized; i.e., $\int d\mathbf{q}_s d\mathbf{q}_{as} |\Phi(\mathbf{q}_s, \mathbf{q}_{as})|^2 = 1$. Notice that, due to the approximations used and discussed above, the explicit use of the parameter w_1 is necessary to obtain a normalized mode function.

Equation (6) describes the spatial quantum state of the Stokes+anti-Stokes pair. *The important point to be considered here is that the specific characteristics of the state depend on the angle of emission.* For a nearly collinear configuration ($\varphi = 1^\circ - 3^\circ$), which is the case in most experimental configurations [4,9,10], the spatial shape of the quantum state shows cylindrical symmetry in the transverse planes (x_s, y_s) and (x_{as}, y_{as}) , since $A = D$ in Eq. (6). This is not generally true for other configurations.

III. ORBITAL ANGULAR MOMENTUM CORRELATIONS

The azimuthal variation of the spatial correlations translate into different OAM correlations between the Stokes and anti-Stokes photons. In order to make it clearer, let us consider the case where the anti-Stokes photon is projected into a Gaussian mode U_g with beam width at the center of the cloud w_g . This can be achieved by detecting the anti-Stokes photon with a single-mode fiber, placed after a conveniently designed optical system. The resulting mode function of the Stokes photon is written $\Phi_s(\mathbf{q}_s) = \int d\mathbf{q}_{as} \Phi(\mathbf{q}_s, \mathbf{q}_{as}) U_g^*(\mathbf{q}_{as})$; then,

$$\Phi_s(\mathbf{q}_s) = \frac{(FG)^{1/4}}{(2\pi)^{1/2}} \exp\left[-\frac{F}{4}(q_s^x)^2 - \frac{G}{4}(q_s^y)^2\right], \quad (8)$$

with

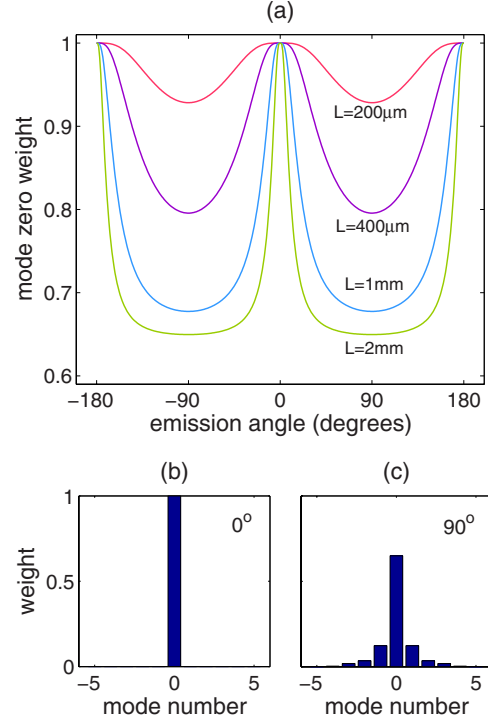


FIG. 2. (Color online) (a) Weight of the OAM mode $m_s=0$ as a function of the emission angle for different values of the length of the cloud of atoms (L). (b) and (c) Two typical OAM distributions of the Stokes photon for $\varphi=0^\circ$ and $\varphi=90^\circ$, respectively. In both cases $L=2$ mm. Data: $w_0=100 \mu\text{m}$, $R=400 \mu\text{m}$, $w_1=100 \mu\text{m}$, and $w_g=500 \mu\text{m}$.

$$\begin{aligned} F &= \frac{4AB + (A+B)w_g^2}{A+B+w_g^2}, \\ G &= \frac{4CD + (C+D)w_g^2}{C+D+w_g^2}. \quad (9) \end{aligned}$$

The mode function of the Stokes photon as given by Eq. (8) can be described by a superposition of OAM modes [17] $\Phi_s(\rho_s, \varphi_s) = (2\pi)^{-1/2} \sum_{m_s} a_{m_s}(\rho_s) \exp(im_s \varphi_s)$, where (ρ_s, φ_s) are cylindrical coordinates in the transverse wave-number domain and m_s is the index of each mode. The weight of each spiral mode, $P_{2m_s} = |a_{2m_s}|^2$, can be found to be

$$\begin{aligned} P_{2m_s} &= (FG)^{1/2} \int \rho_s d\rho_s \exp\left\{-\frac{F+G}{4}\rho_s^2\right\} \\ &\times I_m^2\left[\frac{G-F}{8}\rho_s^2\right], \quad (10) \end{aligned}$$

where I_m is a Bessel function of the second kind.

Figure 2(a) shows the weight of the mode $m_s=0$ as a function of the angle of emission for different values of the length of the cloud of atoms. Figures 2(b) and 2(c) show two typical OAM decompositions. The pump and control beams are Gaussian beams, with $m_c = m_p = 0$, where m_i describes an OAM of $m_i \hbar$ per photon of the corresponding beam. For

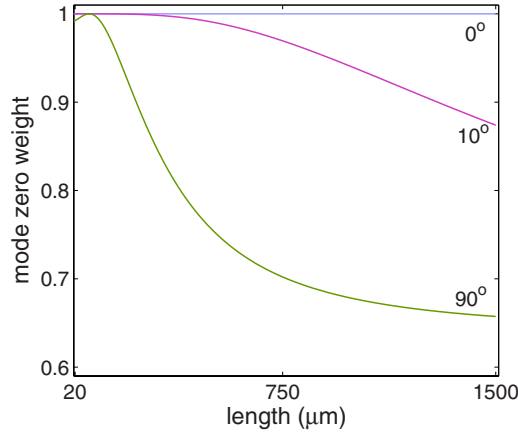


FIG. 3. (Color online) (a) Weight of the OAM mode $m_s=0$ as a function of the length of the cloud, for different values of the emission angle (φ). Data: $w_0=100\ \mu\text{m}$, $R=400\ \mu\text{m}$, $w_1=100\ \mu\text{m}$, and $w_g=500\ \mu\text{m}$.

nearly collinear configuration, Fig. 2 shows that we obtain the expected relationship $m_s=m_{as}$, while this might not be the case for highly noncollinear configurations.

The results of Fig. 2 can be understood if we consider that the effective volume of the interaction is determined by the effective size of the atomic cloud in the longitudinal (L) and transverse planes (R), by the beam waist (w_0) of the pump beam and control beams, and by the size w_1 of the modes of the Stokes and anti-Stokes photons. The spatial mode function shows cylindrical symmetry when $A=D$ in Eq. (6), so that the condition

$$L = \frac{R}{(1 + 2R^2/w_0^2)^{1/2}} \quad (11)$$

is fulfilled. If the beam waist is much larger than the size of the cloud in the transverse dimensions, the condition turns out to be $L=R$.

Under the conditions of Eq. (11), the spatial mode function shows cylindrical symmetry, as for a nearly collinear configuration, but now, *this is true for all possible directions of emission of the paired photons*. Pairs of photons emitted in different directions show the same spatial quantum properties. Any deviation from a spherical-like volume of interaction introduces ellipticity in the mode function and, therefore, azimuthal spatial distinguishing information of pairs of photons emitted in different directions. In [6] the relationship $m_s=m_{as}$ is measured. The authors use a nearly collinear configuration that, as demonstrated here, it should fulfill this relationship. Notwithstanding, we predict that this should not be the case for other noncollinear configurations, as the one used in [5], if the volume of interaction is highly elliptical.

Figure 3 shows the weight of the mode $m_s=0$ as a function of the length of the cloud for different values of the angle of emission. For a collinear configuration, $m_s=m_{as}=0$ for any value of the length of the cloud. When the angle of emission increases, the OAM distribution now depends on the length of the cloud, but the change of the length of the cloud affects very weakly the mode weight when the length of the cloud is much longer than the relevant parameters: w_1 ,

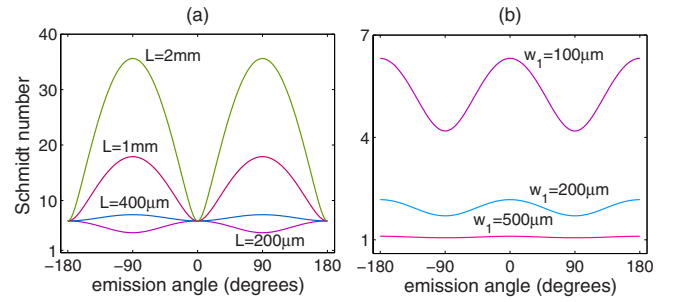


FIG. 4. (Color online) Amount of spatial entanglement (Schmidt number K) of the Stokes+anti-Stokes pair for different angles of emission φ . (a) For various values of the length of the cloud (as indicated by the label). $w_1=100\ \mu\text{m}$. (b) For various values of the pump beam width (as indicated by the label). Length of the cloud: $L=200\ \mu\text{m}$. In both cases, $R=1000\ \mu\text{m}$ and $w_0=500\ \mu\text{m}$.

w_g , and R . This is specially evident for the case of the angle of emission $\varphi=90^\circ$.

IV. SPATIAL ENTANGLEMENT

Let us consider in more detail how it changes the quantum state of different pairs of photons emitted along different directions of propagation. The amount of spatial entanglement embedded in the quantum state can be quantified by the Schmidt number [18] $K=1/\sum_n \lambda_n^2$, where the eigenvalue λ_n comes from the decomposition $\Phi(\mathbf{q}_s, \mathbf{q}_{as}) = \sum_n \sqrt{\lambda_n} f_n(\mathbf{q}_s) g_n(\mathbf{q}_{as})$. Taking into account Eq. (6), one can find that [19,20]

$$K = \frac{(A+B)(C+D)}{4(ABCD)^{1/2}}. \quad (12)$$

Figure 4 shows the value of the Schmidt number as a function of the angle of emission, φ , for different values of the length of the atomic cloud and the filter width. Importantly, the degree of spatial entanglement of the two-photon state shows azimuthal variations, depending on the direction of emission of the Stokes and anti-Stokes photons. For $L < R(1 + 2R^2/w_0^2)^{-1/2}$, as dictated by Eq. (11), the maximum amount of entanglement is achieved for nearly collinear configurations ($\varphi \sim 0^\circ$). In other words, the Schmidt decomposition contains more modes in a nearly collinear configuration, than in a transverse emitting configuration ($\varphi=90^\circ$), showing therefore a higher degree of entanglement. If we increase the length of the cloud, the amount of entanglement decreases, as well as the azimuthal variability of the entanglement. If Eq. (11) is fulfilled, the amount of spatial entanglement is constant for all angles of emission. For $L > R(1 + 2R^2/w_0^2)^{-1/2}$, the maximum amount of entanglement is achieved for transverse emitting configurations. Notice also that strong spatial filtering—i.e., increasing w_1 —also diminishes both the amount of entanglement and its azimuthal variability.

V. CONCLUSIONS

We have shown that pairs of entangled Stokes and anti-Stokes photons, when generated in different directions of

propagation, show different quantum spatial properties due to the presence of ellipticity of the mode function—i.e., *azimuthal spatial distinguishability*. The degree of ellipticity and azimuthal distinguishability depend on the shape of the volume of interaction of the atom-light interactions. It is negligible for nearly collinear configurations and for highly non-collinear configurations in spherical-like clouds of atoms.

The measurement of the ellipticity of the mode function, which would translate in the observation of paired photons with OAM correlations that do not fulfill the relationship $m_s = m_{as}$, is within the availability of current experimental configurations for highly noncollinear configurations, such as transverse emitting configuration [5], when highly elliptical atom clouds are considered. In SPDC configurations, many experimental configurations make use of highly elliptical volumes of interaction. In this regime, the ellipticity of the mode function has already been experimentally verified [11,12].

This effect might have an important impact on the application of quantum information protocols that make use of orbital angular momentum correlations [21]. The azimuthal distinguishing information introduced by the direction of emission can affect the quantum properties of polarization-

entangled photons when these photons are generated with different angles of emission, as is the case in [10]. If the volume of interaction is spherical-like ($R \approx L$), the realization of high-dimensional entanglement by selecting several spatial modes (directions of emission), as proposed in [10], can be achieved without introducing spatial distinguishing information between different pairs of photons, which can degrade the quality of the entanglement generated. On the other hand, the presence of ellipticity of the mode function as a function of the emission angle could restrict the angles of emission accessible for generating a polarization entangled state with a degree of concurrence above a certain prescribed level.

ACKNOWLEDGMENTS

This work was supported by Projects No. FIS2007-60179 and No. FIS2005-03394 and Consolider-Ingenio 2010 Quantum Optical Information Technologies (QOIT), from the Government of Spain, and by the European Commission [Qubit Applications (QAP), Contract No. 015848]. S.B. is on leave from the Universidad de Montevideo.

-
- [1] *The Physics of Quantum Information*, edited by D. Boumeester, A. Ekert, and A. Zeilinger (Springer-Verlag, Berlin, 2000).
- [2] S. Haroche and J. M. Raimond, *Exploring the Quantum: Atoms, Cavities and Photons* (Oxford University Press, Oxford, 2006).
- [3] L. M. Duan, J. I. Cirac, and P. Zoller, Phys. Rev. A **66**, 023818 (2002).
- [4] D. N. Matsukevich, T. Chaneliere, M. Bhattacharya, S.-Y. Lan, S. D. Jenkins, T. A. B. Kennedy, and A. Kuzmich, Phys. Rev. Lett. **95**, 040405 (2005).
- [5] V. Baliç, D. A. Braje, P. Kolchin, G. Y. Yin, and S. E. Harris, Phys. Rev. Lett. **94**, 183601 (2005).
- [6] R. Inoue, N. Kanai, T. Yonehara, Y. Miyamoto, M. Koashi, and M. Kozuma, Phys. Rev. A **74**, 053809 (2006).
- [7] J. H. Eberly, J. Phys. B **39**, S599 (2006).
- [8] M. O. Scully, E. S. Fry, C. H. Raymond Ooi, and K. Wodkiewicz, Phys. Rev. Lett. **96**, 010501 (2006).
- [9] A. Kuzmich, W. P. Bown, A. D. Boozer, A. Boca, C. W. Chou, L.-M. Duan, and H. J. Kimble, Nature (London) **423**, 731 (2003).
- [10] S. Chen, Y. A. Chen, B. Zhao, Z. S. Yuan, J. Schmiedmayer, and J. W. Pan, Phys. Rev. Lett. **99**, 180505 (2007).
- [11] A. R. Altman, K. G. Koprulu, E. Corndorf, P. Kumar, and G. A. Barbosa, Phys. Rev. Lett. **94**, 123601 (2005).
- [12] G. Molina-Terriza, S. Minardi, Y. Deyanova, C. I. Osorio, M. Hendrych, and J. P. Torres, Phys. Rev. A **72**, 065802 (2005).
- [13] C. I. Osorio, G. Molina-Terriza, B. Font, and J. P. Torres, Opt. Express **15**, 14636 (2007).
- [14] J. P. Torres, C. I. Osorio, and L. Torner, Opt. Lett. **29**, 1939 (2004).
- [15] D. A. Braje, V. Baliç, S. Goda, G. Y. Yin, and S. E. Harris, Phys. Rev. Lett. **93**, 183601 (2004).
- [16] J. Wen and M. H. Rubin, Phys. Rev. A **74**, 023808 (2006); **74**, 023809 (2006).
- [17] G. Molina-Terriza, J. P. Torres, and L. Torner, Phys. Rev. Lett. **88**, 013601 (2001).
- [18] A. Ekert and P. L. Knight, Am. J. Phys. **63**, 415 (1995).
- [19] P. S. K. Lee, M. P. van Exter, and J. P. Woerdman, Phys. Rev. A **72**, 033803 (2005).
- [20] K. W. Chan, J. P. Torres, and J. H. Eberly, Phys. Rev. A **75**, 050101(R) (2007).
- [21] G. Molina-Terriza, J. P. Torres, and L. Torner, Nat. Phys. **3**, 305 (2007).